Supplementary information

Flexible NIR-Transparent Perovskite Solar Cells for All-Thin-Film Tandem Photovoltaics Devices

Stefano Pisoni[1], Fan Fu[1], Thomas Feurer[1], Mohammed Makha[2], Benjamin Bissig[1], Shiro Nishiwaki[1], Ayodhya N. Tiwari[1] and Stephan Buecheler[1]**

[1]Laboratory for Thin Films and Photovoltaics, Empa – Swiss Federal Laboratories for Materials Science and Technology, Ueberlandstrasse 129, 8600 Duebendorf, Switzerland

[2]Laboratory for Functional Polymers, Empa – Swiss Federal Laboratories for Materials Science and Technology, Ueberlandstrasse 129, 8600 Duebendorf, Switzerland

* E-mail: stefano.pisoni@empa.ch, stephan.buecheler@empa.ch

Materials:

In_2O_3 (99.99%) and ZnO (99.99%) targets were bought from Plasmaterials (US), and Al doped ZnO (containing 2 wt% Al_2O_3) target was bought from Materion (99.995%). Spiro-OMeTAD was bought from Merck. Lithium-bis(trifluoromethanesulfonyl)imide (Li-TFSI) and 4-tertbutylpyridine (TBP) were bought from Sigma-Aldrich. CH_3NH_3I (powder, ITEM# MS101000) and PbI_2 (ultra-dry, 99.999%, metals basis) were purchased from Dyesol (Australia) and Alfa Aesar, respectively. Fullerene carbon 60 powder (C60) was bought from SES Research (purity > 99.5%). Molybdenum oxide (99.95%, metals basis) was purchased from Alfa Aesar.

All chemicals are used as received without any further treatment for purification.

RF-sputtering of Hydrogenated indium oxide (In_2O_3:H):

In_2O_3:H layers were deposited in a high vacuum sputtering system (AJA Intl.) by RF-sputtering of ceramic In_2O_3 (99.99%) targets at an applied sputter power density of 3.0 W/cm^2 without intentional heating of the substrate. The reactive atmosphere consisted of a gas mixture of Ar, O_2, and H_2O at a total pressure of 0.6 Pa. H_2O vapor for H doping was injected via a needle valve with a partial pressure of ~1 x 10^{-4} Pa.

Atomic Force Microscopy (AFM):

The morphology images were acquired using AFM Bruker ICON in PeakForce QNM mode (based on PeakForce Tapping technology).

X-ray diffraction (XRD) measurements:

X-ray diffraction patterns were obtained in Bragg-Brentano geometry by using a X'Pert PRO θ-2θ scan (Cu-$K_{\alpha 1}$ radiation, λ = 1.5406 Å) from 10 to 60° (2θ) with a step interval of 0.0167°.

Scanning Electron Microscopy (SEM):

The cross sectional images of the samples were investigated with a Hitachi using 5 kV voltage and 10 mA. A thin layer of Pt was coated on top of the sample to avoid charging effect.

UV-Visible spectroscopy:

The transmission (*T*) and reflection (*R*) spectra were acquired using a UV-Vis-NIR spectrophotometer (Shimadzu UV-3600) equipped with an integrating sphere. Absorption *A* is calculated using the following formula: $A=1-T-R$.

Time resolved photoluminescence (TRPL)

For time resolved photoluminescence (TRPL) measurements, a 639 nm diode laser with pulse duration of 92 ps was used as excitation source. Pulse repetition rates were around 1 MHz and the number of photons per area and pulse was approximately 1×10^{13} photons cm^{-2}. The spectrally integrated luminescence decay was measured using a Picoquant PMA-C 192-M photomultiplier time and a Picoquant TimeHarp 260 digitizing system with 50 ps time channel width.

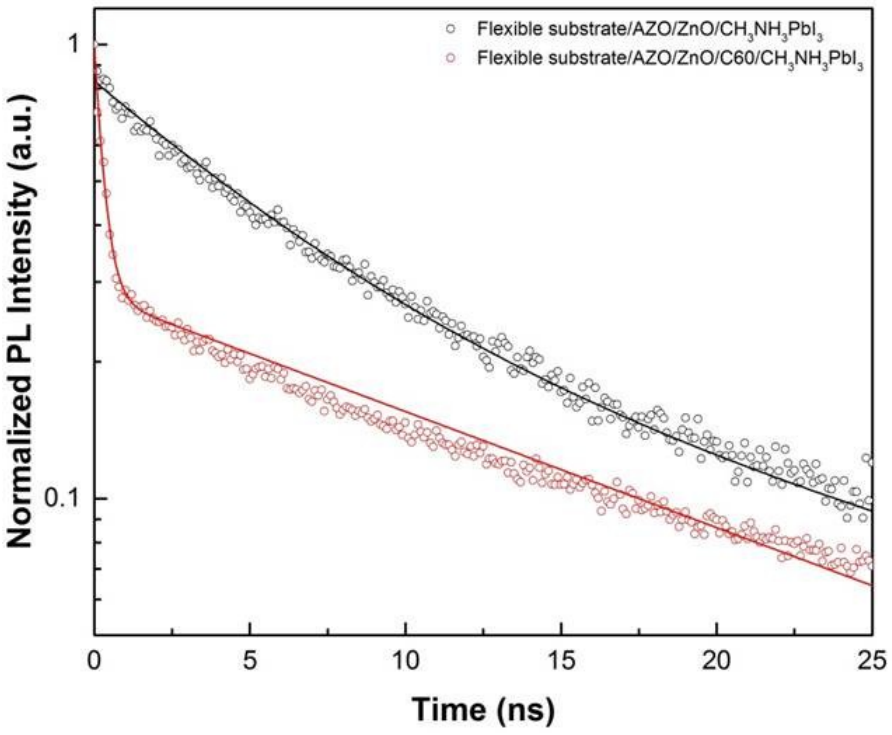

Fig. S1 Comparison between TRPL spectra of $CH_3NH_3PbI_3$ films on ZnO/AZO and C60/ZnO/AZO substrates. TRPL data are fitted by a bi-exponential decay function containing a fast decay and a slow decay process. The fast decay lifetimes for $CH_3NH_3PbI_3$ grown on ZnO and C60 are 6 ns and 0.3 ns, respectively.

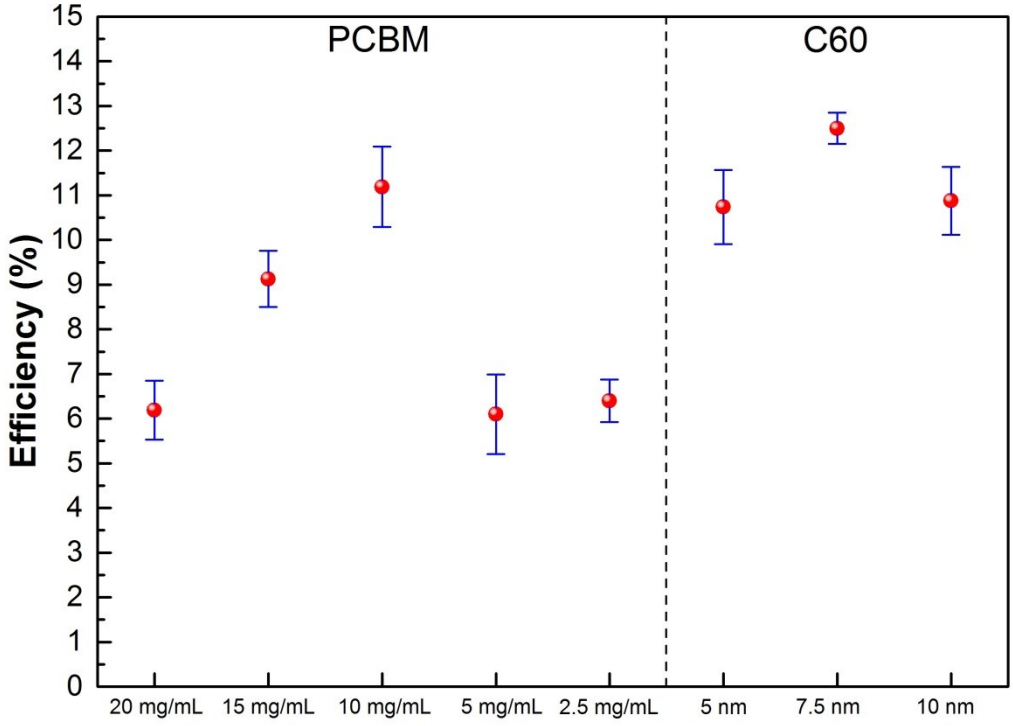

Fig. S2 Comparison of efficiencies with five different PCBM concentrations in chlorobenzene (20, 15, 10, 5 and 2.5 mg mL^{-1}) and three different thermally evaporated C60 thicknesses (5, 7.5 and 10 nm). Mean values are represented by red spots, the error bars represent one standard deviation from the mean.

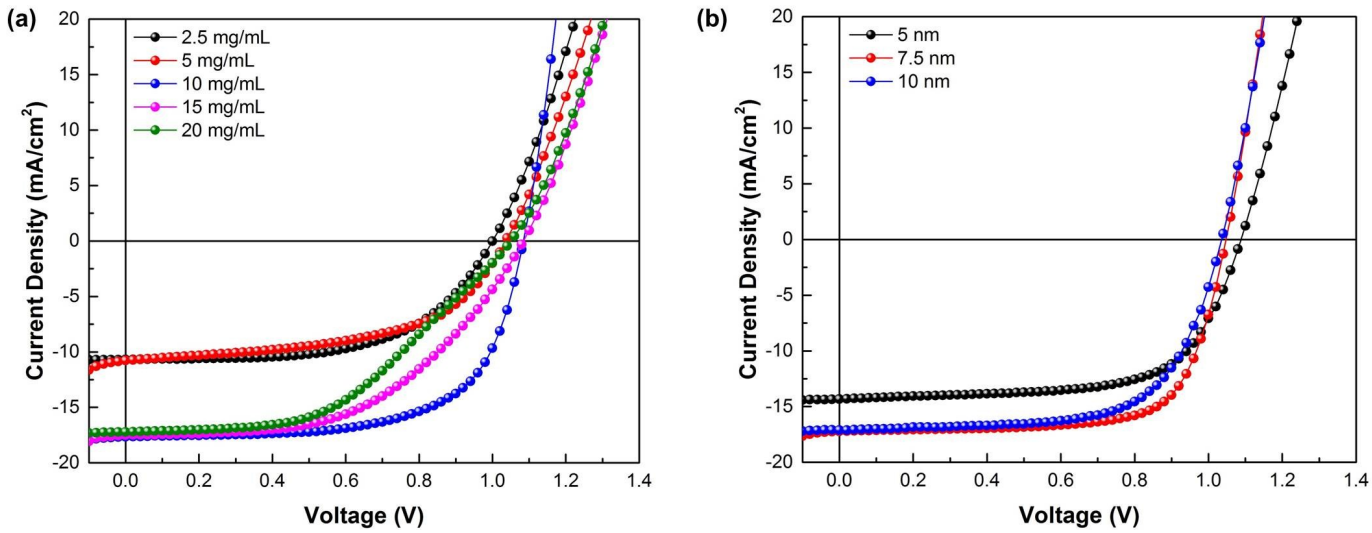

Fig. S3 a) most representative *J-V* curves of the samples batch, under forward voltage scanning, for different PCBM concentrations. b) most representative *J-V* curves of the samples batch, under forward voltage scanning, for different thermally evaporated C60 thicknesses.

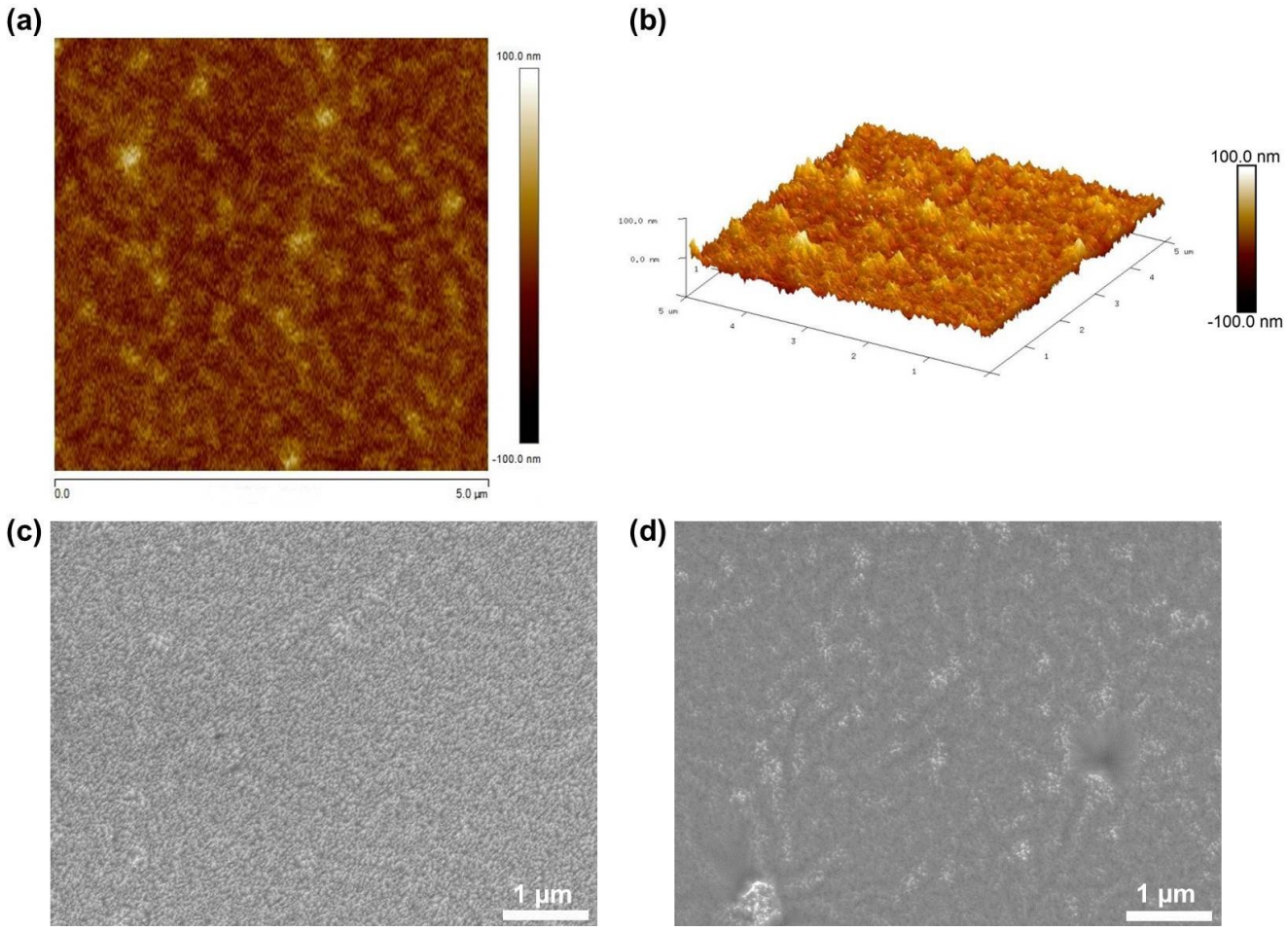

Fig. S4 a) AFM measurement of sputtered ZnO surface on top of AZO, root mean square roughness of 10.9 nm. b) 3D AFM view of the ZnO surface on top of AZO. c) Top view SEM image of sputtered ZnO surface. d) Top view SEM image of ZnO surface coated with PCBM. The coating does not seem perfectly uniform, some "lighter" regions are observed, possible non coated ZnO peaks.

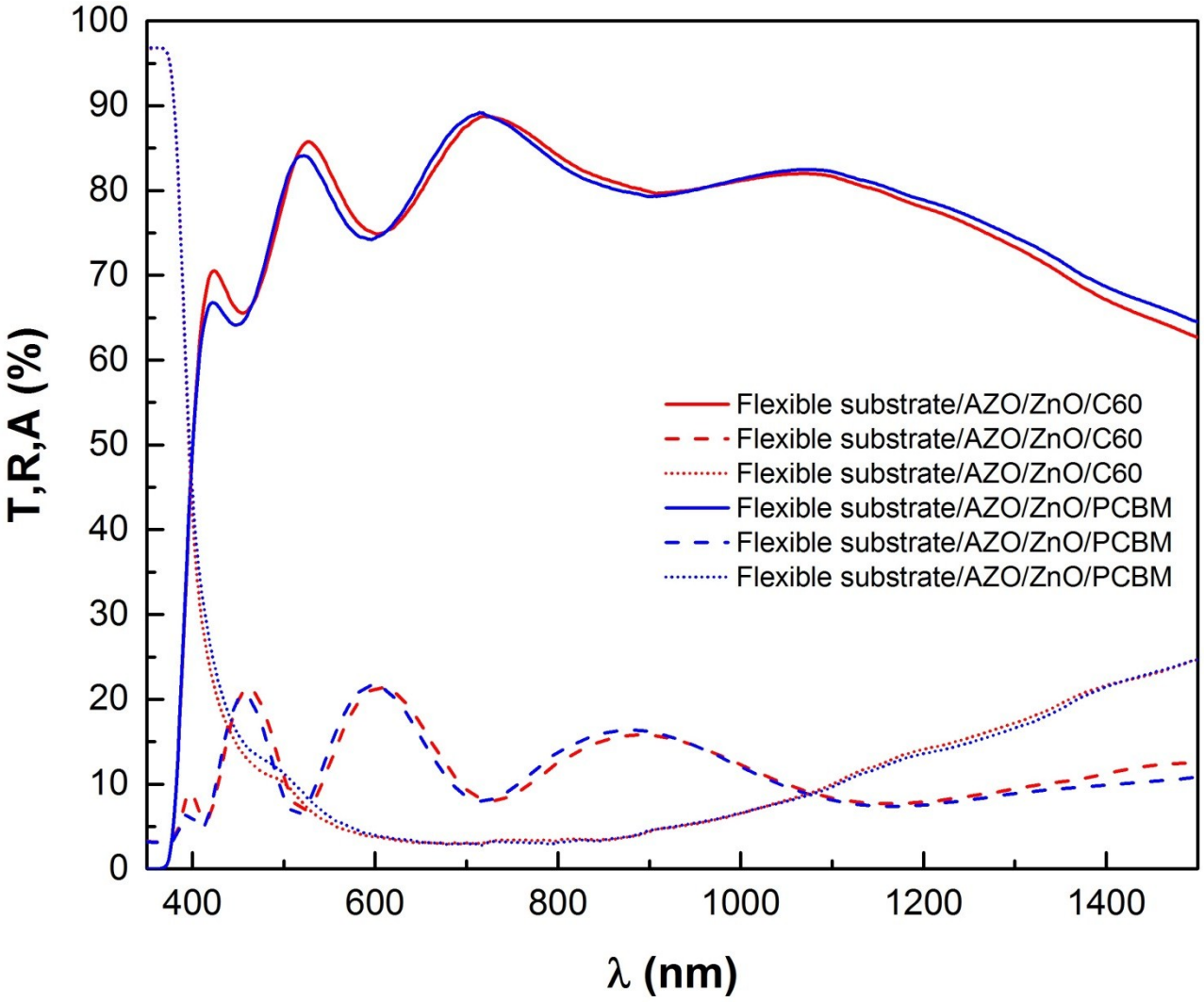

Fig. S5 Optical properties (Transmittance, solid lines, reflectance, dashed lines and absorptance, dotted lines) of Flexible substrate/AZO/ZnO/C60 (red lines) and of Flexible substrate/AZO/ZnO/PCBM (blue lines) substrates, measured by UV-vis-NIR spectroscopy.

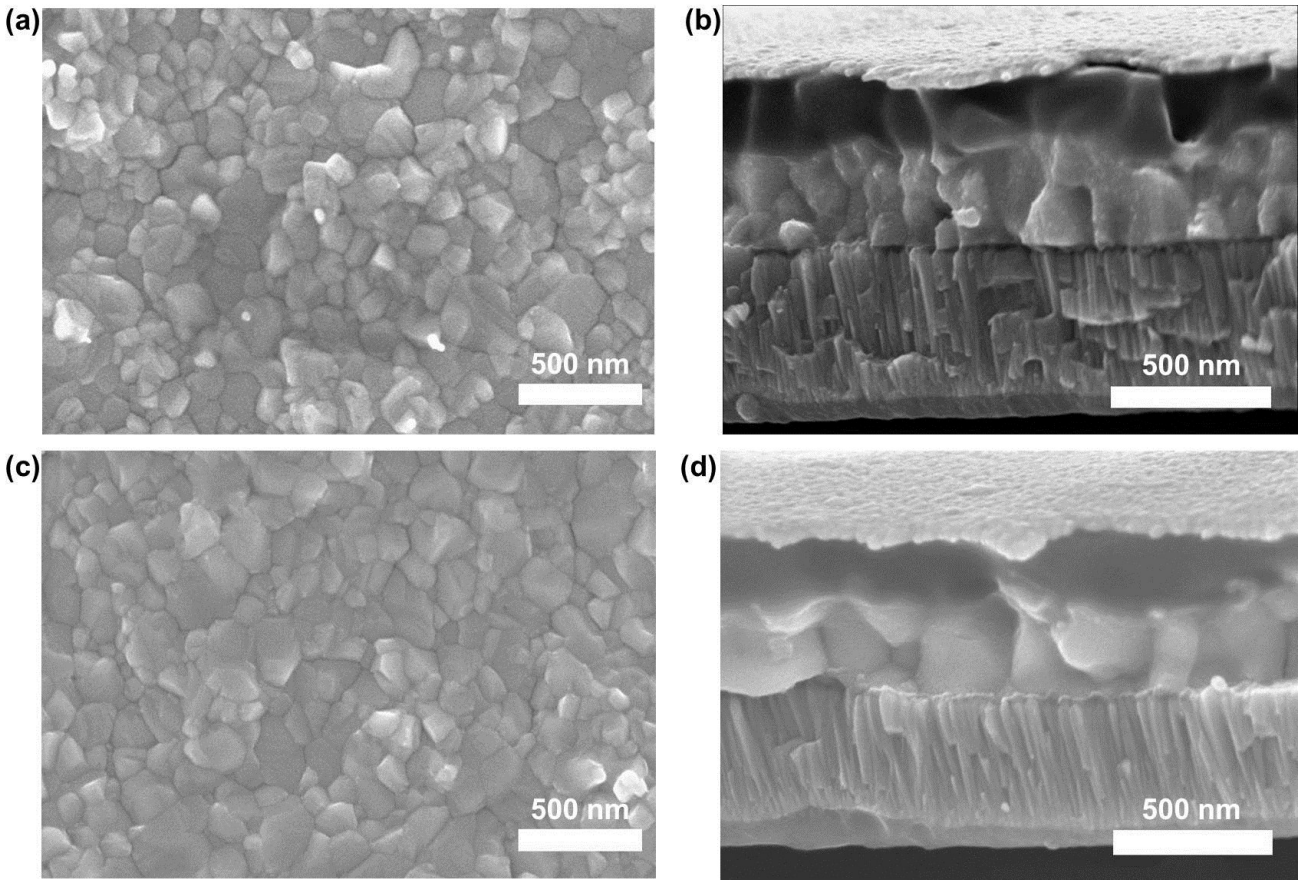

Fig. S6 a) Top view SEM image of $CH_3NH_3PbI_3$ grown on spin coated PCBM film. b) Cros section image of complete device based on spin coated PCBM. c) Top view SEM image of $CH_3NH_3PbI_3$ grown on thermally evaporated C60 film. d) Cross section image of complete device based on thermally evaporated C60.

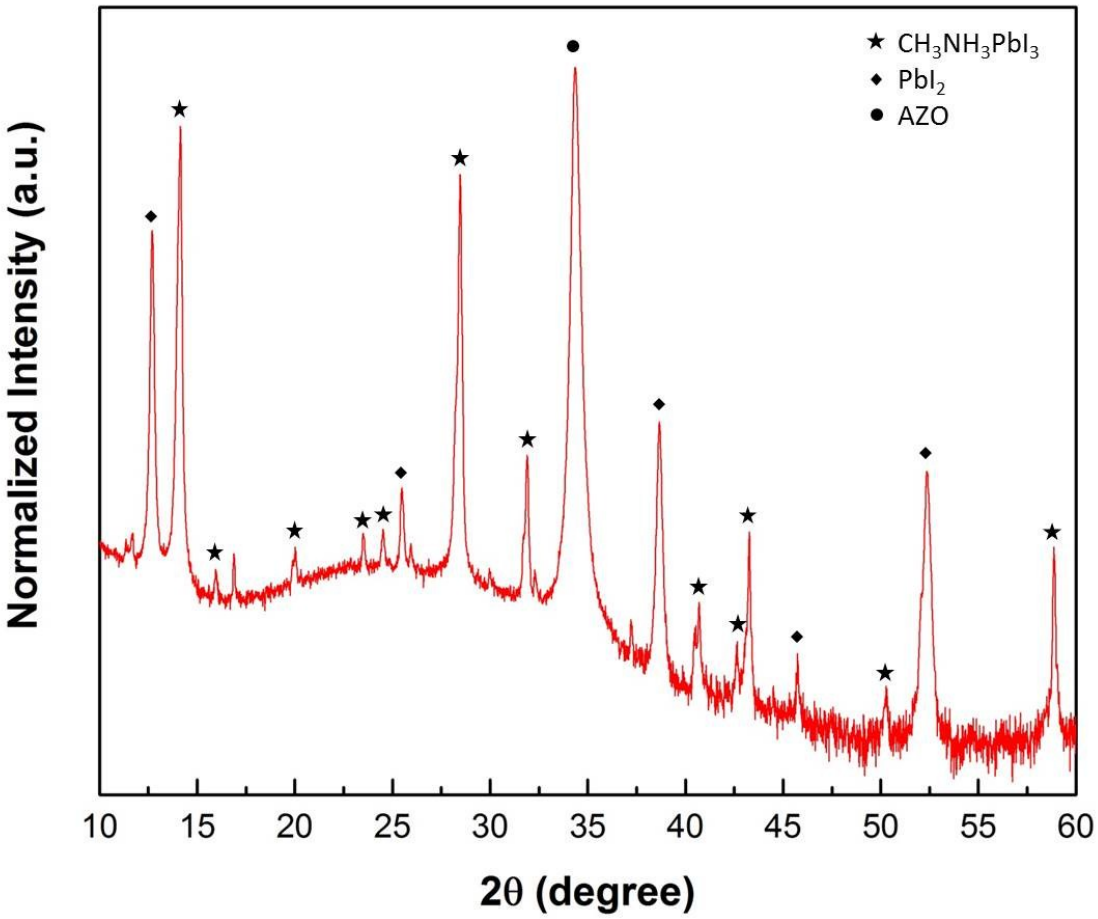

Fig. S7 XRD spectrum of perovskite grown by two-step deposition on top of Glass/AZO/ZnO/C60 substrate. A certain amount of unreacted PbI_2 can be observed after perovskite thermal annealing (50° for 1 hour).

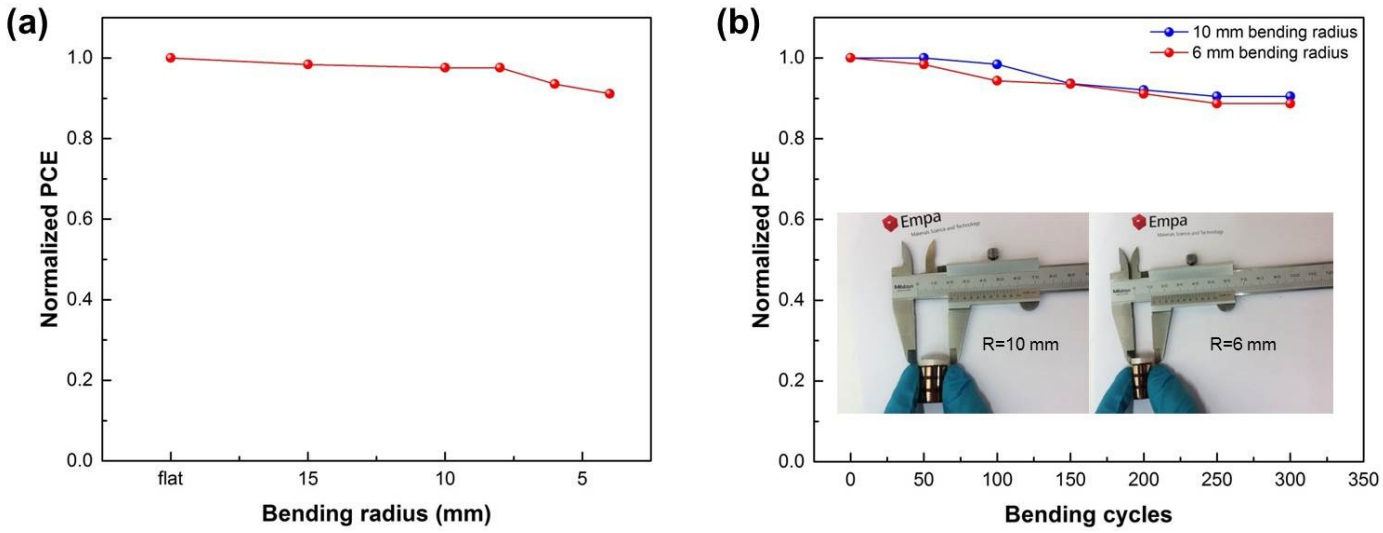

Fig. S8 a) Normalized power conversion efficiencies (PCEs) for one cycle bending tests at different curvature radii (flat, 15, 10, 8, 6 and 4 mm). More than 91% of the original efficiency is retained after 4 mm bending. b) Normalized PCEs as a function of bending cycles at fixed bending radii of 10 and 6 mm. More than 90% and 88% of the original efficiency is retained after 300 bending cycles at 10 mm and 6 mm bending radius, respectively. The inset shows the flexible devices bent at 10 and 6 mm using a Vernier caliper to define the bending radius.

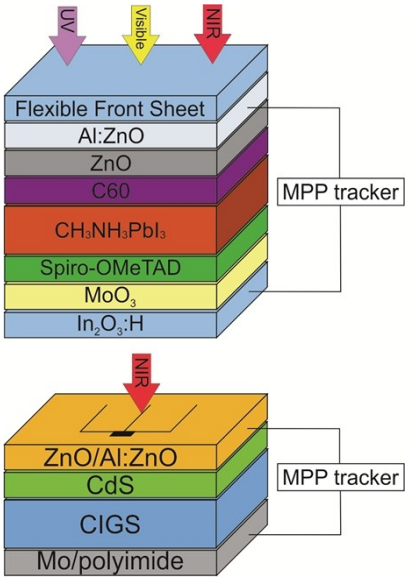

Fig. S9 Schematic representation of the 4-terminal tandem configuration, employing flexible CIGS and perovskite sub-cells.